Hydrodynamic stability of a suspension in cylindrical Couette flow

Mohamed E. Ali
Mechanical Engineering Department, King Saud University, P.O. Box 800, Riyadh 11421, Saudi Arabia

Deepanjan Mitra, John A. Schwille, and Richard M. Lueptow
Department of Mechanical Engineering, Northwestern University, Evanston, Illinois 60208

(Received 8 October 2001; accepted 11 December 2001)

A linear stability analysis was carried out for a dilute suspension of rigid spherical particles in cylindrical Couette flow. The perturbation equations for both the continuous fluid phase and the discontinuous particle phase were decomposed into normal modes resulting in an eigenvalue problem that was solved numerically. At a given radius ratio, the theoretical critical Taylor number at which Taylor vortices first appear decreases as the particle concentration increases. Increasing the ratio of particle density to fluid density above one decreases the stability. However, using an effective Taylor number based on the suspension density and viscosity largely accounts for this effect. The axial wave number is the same for a suspension as it is for a pure fluid. Experiments using neutrally buoyant particles in a Taylor–Couette apparatus show that the flow is more stable as the particle concentration increases. The reason that the theory does not fully capture the physics of the flow should be addressed in future research.
[DOI: 10.1063/1.1449468]

I. INTRODUCTION

The linear stability of circular Couette flow in the annulus between a rotating inner cylinder and a concentric, fixed outer cylinder has been studied from both theoretical and experimental standpoints. The instability appears as pairs of counter-rotating, toroidal vortices stacked in the annulus. Taylor[1] conducted a simple flow visualization experiment to confirm his analytic prediction for the onset of the instability. Chandrasekhar,[2] DiPrima and Swinney,[3] Kataoka,[4] and Koschmeider[5] provide extensive summaries of the abundant research on this topic since Taylor's pioneering work.

The stability of Taylor vortex flow is altered when complexity is added to the system. For instance, an axial flow in the annulus stabilizes the circular Couette flow so that the transition to supercritical Taylor vortex flow occurs at a higher Taylor number.[6–8] Likewise, a radial flow in the annulus between differentially rotating porous cylinders also affects the stability of the Taylor vortex flow.[9–11]

Our interest in the effect of a complex fluid, specifically a dilute suspension, on the stability of Taylor–Couette flow is motivated by the processing of a suspension in a Taylor–Couette reactor cell[12–15] or in a rotating filter device during dynamic filtration.[16–24] In Taylor–Couette reactors, chemically reacting species are dispersed or exposed uniformly to chemical catalysts by the vortical motion. In rotating filter devices, an axial flow introduces a suspension into the annulus between a rotating porous inner cylinder and a stationary nonporous outer cylinder. Filtrate passes radially through the porous wall of the rotating inner cylinder, while the concentrate is retained in the annulus. The Taylor vortices appearing in the device are believed to wash the filter surface of the inner cylinder clean of particles thus preventing the plugging of pores of the filter medium.[25] Centrifugal forces acting on the particles in suspension and the shear resulting from the rotation of the inner cylinder are also thought to inhibit particles from plugging the pores of the filter.[26]

Nearly all research on the stability of cylindrical Couette flow has been done for simple Newtonian fluids with a few notable exceptions. Recently there has been interest in the stability of a viscoelastic fluid in Taylor–Couette flow.[27] For example, using a simple viscoelastic constitutive equation, Khayat found that the flow is destabilized as the fluid elasticity is increased.[28] However, experimental results indicate both stabilizing and destabilizing effects of viscoelasticity, depending upon the polymer solution used.[29] Fewer studies have addressed a suspension as a complex fluid in cylindrical Couette flow. Nsom carried out a stability analysis for a suspension of rigid fibers using rheological coefficients in the stress tensor to account for the non-Newtonian effects.[30] Results indicate that increasing the concentration of fibers increases the stability of the system. Yuan and Ronis considered the stability of colloidal crystals in cylindrical Couette flow using a Stokes drag interaction between the particles and the fluid.[31] Although the Taylor instability is suppressed as the colloidal crystal lattices become more rigid, other lattice instabilities appear. Although not directly related to the stability of a suspension, there recently has been substantial interest in tracking particle motion in both nonwavy and wavy Taylor–Couette flow.[32–37] This work has focused on particle paths and enhanced diffusion without regard to the effect of the particles in the suspension on the stability of the flow. Finally, Dominguez-Lerma *et al.* detected a nonperiodically time-dependent nonuniformity in the size of the vortices when a low concentration of flakes was used to visualize Taylor–Couette flow in vertical apparatus, but they did not note how the flakes affected the critical Taylor number.[38]

The processing of suspensions in Taylor–Couette reactor cells and in rotating filtration devices has motivated us to address the effect of particles on the stability of Taylor–

Couette flow. In this study we apply linear hydrodynamic stability analysis to determine the critical Taylor number for the transition from stable cylindrical Couette flow to vortical flow when a dilute concentration of a discontinuous phase of rigid spherical particles is present in the fluid. In addition, we provide results of simple experiments on the stability of a suspension of neutrally buoyant particles in cylindrical Couette flow. While the stability of the flow of a suspension in a Taylor–Couette device is a much simpler problem than that in a Taylor–Couette reactor cell or in a rotating filtration device that have axial flow and other complications, our intent is to provide insight into the stability of the flow in these devices.

II. ANALYTICAL FORMULATION

The conservation equations for the system are based on the traditional two-fluid formulation, appropriate for a dilute concentration of monodisperse rigid particles.[39] In this formulation, concentration-weighted forms of the continuity and Navier–Stokes equations in cylindrical coordinates (r,θ,z) are used for the continuous fluid phase and the disperse particle phase. The flow is assumed to be steady and incompressible. The cylinders are assumed to be infinitely long with the inner cylinder rotating and the outer cylinder fixed. For axisymmetric flow, the dimensional form of the continuity and Navier–Stokes equations for the fluid phase are

$$\frac{1}{r^*}\frac{\partial}{\partial r^*}(r^*V^*_{fr})+\frac{\partial V^*_{fz}}{\partial z^*}=0, \tag{1a}$$

$$\frac{\partial V^*_{fr}}{\partial t^*}+V^*_{fr}\frac{\partial V^*_{fr}}{\partial r^*}-\frac{V^{*2}_{f\theta}}{r^*}+V^*_{fz}\frac{\partial V^*_{fr}}{\partial z^*} =\nu\left[\frac{\partial}{\partial r^*}\left(\frac{1}{r^*}\frac{\partial}{\partial r^*}(r^*V^*_{fr})\right)+\frac{\partial^2 V^*_{fr}}{\partial z^{*2}}\right]-\frac{1}{\rho_f}\frac{\partial p^*}{\partial r^*}-\frac{nF^*_r}{\rho_f}, \tag{1b}$$

$$\frac{\partial V^*_{f\theta}}{\partial t^*}+V^*_{fr}\frac{\partial V^*_{f\theta}}{\partial r^*}+\frac{V^*_{fr}V^*_{f\theta}}{r^*}+V^*_{fz}\frac{\partial V^*_{f\theta}}{\partial z^*} =\nu\left[\frac{\partial}{\partial r^*}\left(\frac{1}{r^*}\frac{\partial}{\partial r^*}(r^*V^*_{f\theta})\right)+\frac{\partial^2 V^*_{f\theta}}{\partial z^{*2}}\right]-\frac{nF^*_\theta}{\rho_f}, \tag{1c}$$

$$\frac{\partial V^*_{fz}}{\partial t^*}+V^*_{fr}\frac{\partial V^*_{fz}}{\partial r^*}+V^*_{fz}\frac{\partial V^*_{fz}}{\partial z^*}=\nu\left[\frac{1}{r^*}\frac{\partial}{\partial r^*}\left(r^*\frac{\partial V^*_{fz}}{\partial r^*}\right)+\frac{\partial^2 V^*_{fz}}{\partial z^{*2}}\right] -\frac{1}{\rho_f}\frac{\partial p^*}{\partial z^*}-g-\frac{nF^*_z}{\rho_f}. \tag{1d}$$

In these equations, the asterisk indicates dimensional variables. $(V^*_{fr},V^*_{f\theta},V^*_{fz})$ are the fluid velocities in the r^*, θ^*, and z^* directions, respectively, t^* represents time, p^* is the pressure, ρ_f is the fluid density, n is the number density of the particles, and F^* is defined shortly. The equations for the particulate phase take on a similar form except that the viscous terms are absent. The dimensional form of the continuity and Navier–Stokes equations for the particulate phase are

$$\frac{\partial \alpha_p}{\partial t^*}+\frac{1}{r^*}\frac{\partial}{\partial r^*}(\alpha_p r^* V^*_{pr})+\frac{\partial(\alpha_p V^*_{pz})}{\partial z^*}=0, \tag{2a}$$

$$\frac{\partial V^*_{pr}}{\partial t^*}+V^*_{pr}\frac{\partial V^*_{pr}}{\partial r^*}-\frac{V^{*2}_{p\theta}}{r^*}+V^*_{pz}\frac{\partial V^*_{pr}}{\partial z^*}=-\frac{1}{\rho_p}\frac{\partial p^*}{\partial r^*}+\frac{nF^*_r}{\alpha_p\rho_p}, \tag{2b}$$

$$\frac{\partial V^*_{p\theta}}{\partial t^*}+V^*_{pr}\frac{\partial V^*_{p\theta}}{\partial r^*}+\frac{V^*_{pr}V^*_{p\theta}}{r^*}+V^*_{pz}\frac{\partial V^*_{p\theta}}{\partial z^*}=\frac{nF^*_\theta}{\alpha_p\rho_p}, \tag{2c}$$

$$\frac{\partial V^*_{pz}}{\partial t^*}+V^*_{pr}\frac{\partial V^*_{pz}}{\partial r^*}+V^*_{pz}\frac{\partial V^*_{pz}}{\partial z^*}=-\frac{1}{\rho_p}\frac{\partial p^*}{\partial z^*}-g+\frac{nF^*_z}{\alpha_p\rho_p}, \tag{2d}$$

where $(V^*_{pr},V^*_{p\theta},V^*_{pz})$ are the particle velocities, ρ_p is the particle density, and α_p is the volume fraction of particles. α_f is the volume fraction of the fluid such that $\alpha_f+\alpha_p=1$. We consider very dilute suspensions $(\alpha_f \gg \alpha_p)$, so α_f can be assumed constant and approximately equal to unity. It therefore does not appear in the fluid phase equations. Note that the volume fraction of particles is related to the number density by[40]

$$\alpha_p=\frac{n\pi\phi^{*3}}{6},$$

where ϕ^* is the diameter of the particle. The last term on the right-hand side of the momentum equations for both phases is the Stokes drag and added mass, expressed as

$$F^*_i=3\pi\mu\phi^*(V^*_{fi}-V^*_{pi})+\frac{\rho_f\pi(\phi^*)^3}{12}\frac{\partial}{\partial t^*}(V^*_{fi}-V^*_{pi}) \quad \text{for } i=r,\theta,z, \tag{3}$$

where μ is the dynamic viscosity of the carrier fluid.[41] The drag force acting on the particles due to the fluid is equal in magnitude but has opposite sense to the force acting on the fluid due to the particles, thus coupling the fluid phase and particle phase equations.

The equations are nondimensionalized by using the following scheme:

$$r=\frac{r^*}{d},\quad z=\frac{z^*}{d},\quad \phi=\frac{\phi^*}{d},$$
$$\frac{V_{jr}}{V^*_{jr}}=\frac{V_{j\theta}}{V^*_{j\theta}}=\frac{V_{jz}}{V^*_{jz}}=\frac{1}{\Omega_1 r_1}\quad (\text{where } j=f,p), \tag{4}$$
$$p=\frac{p^*}{\rho_f\Omega_1^2 r_1^2},\quad t=\frac{t^*}{\tau}.$$

Here, the characteristic length scale is the gap width between the two cylinders $d=r_2-r_1$, where r_1 and r_2 are the inner and outer radii of the cylinders, respectively. The velocities are nondimensionalized using the characteristic velocity of rotation $\Omega_1 r_1$ where Ω_1 is the rotational speed of the inner cylinder. $\tau=d^2/\nu$ is the characteristic viscous time scale of the problem. Upon nondimensionalizing the continuity and Navier–Stokes equations the parameters that appear are the density ratio, $\epsilon=\rho_p/\rho_f$, and the Taylor number, $\mathrm{Ta}=\Omega_1 r_1 d/\nu$, where ν is the kinematic viscosity of the carrier fluid. This form of the Taylor number, often called the rotating Reynolds number, is used because it is simple and consistent with the form used in other studies.[42]

The nondimensional equations are similar to those used by Dimas and Kiger to analyze the linear stability of a particle-laden mixing layer.[40] Implicit in this derivation are the following assumptions: (1) The scale of the particle motion relative to the fluid motion is very small. (2) The particle Reynolds number is always less than unity, so that the drag force on the particle is described by Stokes law. (3) The particles are spherical and rigid. (4) The suspension is sufficiently dilute to prevent hydrodynamic interactions between particles. (5) The Faxen correction to the Stokes drag is negligible. (6) The Bassett history force is negligible in comparison to the Stokes drag.

A linear stability analysis is performed by separating the variables into mean and perturbation components such that

$$\begin{aligned} &V_{fr}=u'(r,z,t), \quad V_{f\theta}=\overline{V}(r)+v'(r,z,t),\\ &V_{fz}=w'(r,z,t),\\ &V_{pr}=u'_p(r,z,t), \quad V_{p\theta}=\overline{V}(r)+v'_p(r,z,t),\\ &V_{pz}=w'_p(r,z,t),\\ &p=P+p'(r,z,t), \quad \alpha_p=A+a'_p(r,z,t). \end{aligned} \tag{5}$$

Here, the primed ($'$) variables are the perturbation components, A is the concentration of particles in the undisturbed state, and the stable velocity profile is given by $\overline{V}(r)=C_1 r+C_2/r$, where the constants C_1 and C_2 are functions of the radius ratio, $\eta=r_1/r_2$.

Next, the perturbations are expressed as normal modes of the form

$$\begin{aligned} &\frac{u'}{u(r)}=\frac{v'}{v(r)}=\frac{w'}{w(r)}=e^{(ikz+\sigma t)},\\ &\frac{u'_p}{u_p(r)}=\frac{v'_p}{v_p(r)}=\frac{w'_p}{w_p(r)}=e^{(ikz+\sigma t)},\\ &\frac{p'}{\omega(r)}=e^{(ikz+\sigma t)}, \quad \frac{a'_p}{a_p(r)}=e^{(ikz+\sigma t)}, \end{aligned} \tag{6}$$

where $u(r)$, $v(r)$, $w(r)$, $u_p(r)$, $v_p(r)$, $w_p(r)$, $\omega(r)$, and $a_p(r)$ are the amplitudes of the corresponding disturbances, k is the axial wave number of the disturbance, and $\sigma=\sigma_r+i\sigma_i$ is an amplification factor. The wave number and the amplification factor are nondimesionalized as $k=k^*d$ and $\sigma=\sigma^*\tau$.

Equations (5) and (6) are then substituted into the nondimensionalized governing equations and the stable flow terms subtracted out. Linearization of the equations by discarding higher order terms results in the final form of the disturbance equations, which for the fluid phase can be written as

$$D_*u(r)=-ikw(r), \tag{7a}$$

$$\left(DD_*-k^2-\sigma-\left(\frac{18A}{\phi^2}+\frac{A\sigma}{2}\right)\right)u(r)+2Ta\frac{\overline{V}}{r}v(r) =\mathrm{Ta}(D\omega(r))-\left(\frac{18A}{\phi^2}+\frac{A\sigma}{2}\right)u_p(r), \tag{7b}$$

$$\left(DD_*-k^2-\sigma-\left(\frac{18A}{\phi^2}+\frac{A\sigma}{2}\right)\right)v(r)-\mathrm{Ta}(D_*\overline{V})u(r) =-\left(\frac{18A}{\phi^2}+\frac{A\sigma}{2}\right)v_p(r), \tag{7c}$$

$$\left(DD_*-k^2-\sigma+\frac{1}{r^2}-\left(\frac{18A}{\phi^2}+\frac{A\sigma}{2}\right)\right)w(r) =ik\ \mathrm{Ta}\ \omega(r)-\left(\frac{18A}{\phi^2}+\frac{A\sigma}{2}\right)w_p(r), \tag{7d}$$

where the differential operators D and D_* are defined as

$$D(\ )=\frac{d}{dr}(\ ), \quad D_*(\ )=\frac{d}{dr}(\ )+\frac{1}{r}(\ ).$$

For the case of zero concentration $(A=0)$, these equations reduce to those for Taylor–Couette flow of a simple fluid.[2]

A similar treatment of the particulate phase equations results in expressions for $u_p(r)$, $v_p(r)$, and $w_p(r)$ in terms of the fluid velocity perturbations,

$$\begin{aligned} u_p(r)=&\left\{\frac{2\ \mathrm{Ta}\,\overline{V}P_0}{r((\sigma+P_0)^2+2\ \mathrm{Ta}^2((V/r)D_*V))}\right\}v(r)\\ &+\left\{\frac{P_0(\sigma+P_0)}{((\sigma+P_0)^2+2\ \mathrm{Ta}^2((V/r)D_*V))}\right\}u(r)\\ &-\left\{\frac{\mathrm{Ta}(\sigma+P_0)}{\epsilon((\sigma+P_0)^2+2\ \mathrm{Ta}^2((V/r)D_*V))}\right\}D\omega(r), \end{aligned} \tag{8a}$$

$$\begin{aligned} v_p(r)=&-\left\{\frac{\mathrm{Ta}\,P_0D_*\overline{V}}{((\sigma+P_0)^2+2\ \mathrm{Ta}^2((V/r)D_*V))}\right\}u(r)\\ &+\left\{\frac{P_0(\sigma+P_0)}{((\sigma+P_0)^2+2\ \mathrm{Ta}^2((V/r)D_*V))}\right\}v(r)\\ &+\left\{\frac{\mathrm{Ta}^2\,D_*\overline{V}}{\epsilon((\sigma+P_0)^2+2\ \mathrm{Ta}^2((V/r)D_*V))}\right\}D\omega(r), \end{aligned} \tag{8b}$$

$$w_p(r)=\frac{P_0}{(\sigma+P_0)}w(r)-\frac{ik\,\mathrm{Ta}}{\epsilon(\sigma+P_0)}\omega(r), \tag{8c}$$

where

$$P_0=\frac{18}{\phi^2\epsilon}+\frac{\sigma}{2\epsilon}.$$

The particle velocity components (8) are then substituted into (7) and the equations simplified to a set of 12 nonlinear first-order ordinary differential equations. This system of equations was solved using the boundary-value problem software package SUPORT[43] in combination with the nonlinear equation solver SNSQE.[44,45] Computations were performed in double precision. Extensive code testing of the SUPORT pack-

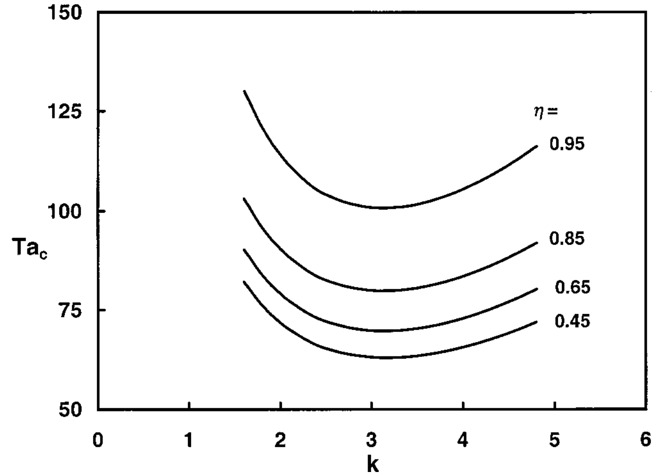

FIG. 1. Sample of the stability curves for several radius ratios ($A=0.05$, $\epsilon=1$, $\phi=0.004$).

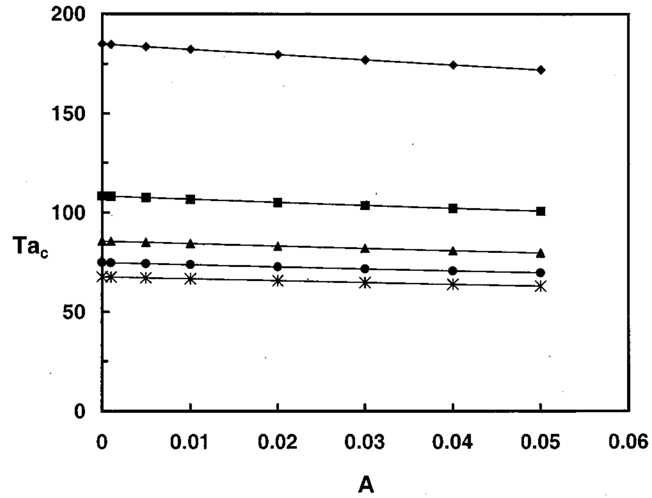

FIG. 2. Critical Taylor number for several radius ratios as a function of particle concentration A for neutrally buoyant particles ($\epsilon=1$, $\phi=0.004$). (*) $\eta=0.45$, (●) $\eta=0.65$, (▲) $\eta=0.75$, (■) $\eta=0.85$, (♦) $\eta=0.95$.

age with the SNSQE solver has been previously reported.[46–49] The eigenvalue problem may be written in the implicit functional form

$$F(\mathrm{Ta}, A, \phi, k, \epsilon, \eta, \sigma) = 0. \tag{9}$$

The parameters A, ϕ, k, ϵ, and η are usually fixed and solution of the ordinary differential equations is obtained by iteration on the eigenvalue pair (Ta, σ_i) using the procedure outlined in Ali and Weidman.[48,49] Since we seek to find the neutral stability conditions, σ_r is set to zero. At fixed radius ratio η, a search is conducted over all wave numbers k to find the minimum Taylor number, denoted as Ta_c. A sample of neutral stability curves for $\eta=0.45$, 0.65, 0.75, and 0.85 are given in Fig. 1 for $A=0.05$, $\epsilon=1$, and $\phi=0.004$. For specific values of A, ϵ, ϕ, and η, critical conditions Ta_c, k_c, and $(\sigma_i)_c$ are those for which the Taylor number is a minimum. For the example in Fig. 1, $\mathrm{Ta}_c=63.04$, 69.75, 79.82, 100.79 in an ascending order of η. In the vicinity of the minimum, the increments in Δk were taken to be 0.001. The wave number of the neutral curves in Fig. 1 are 3.172, 3.143, 3.135, 3.130 in ascending order of η.

To assure the validity of our procedure we compared our results for a simple fluid by assuming zero concentration in the analysis ($A=0$) to previously published results.[50] The similarity of the values for the critical Taylor numbers Ta_c and critical wave numbers k_c, shown in Table I, confirm the validity of our procedure. The critical Taylor number and wave number for Taylor–Couette flow of a simple fluid are also recovered for ϵ approaching zero, corresponding to inertialess particles, further confirming the validity of our numerics.

TABLE I. Comparison of critical Taylor number and wave number obtained for pure Taylor–Couette flow from Rectenwald *et al.* (Ref. 50) with the present study.

η	Ta_c (Ref. 50)	Ta_c (present study)	k_c (Ref. 50)	k_c (present study)
0.400	68.2963	68.2965	3.1835	3.183
0.500	68.1860	68.1863	3.1625	3.162
0.600	71.7154	71.7157	3.1483	3.148
0.700	79.4903	79.4907	3.1389	3.139
0.750	85.7760	85.7765	3.1354	3.135
0.800	94.7331	94.7336	3.1326	3.133
0.900	131.6139	131.6145	3.1288	3.129
0.975	260.9483	260.9499	3.1270	3.127

The range of parameters that was considered is consistent with physically realizable systems. Particle density ratios were used that are consistent with gas bubbles in a liquid ($\epsilon=0.001$), neutrally buoyant particles ($\epsilon=1$), heavy particles in a liquid ($\epsilon=10$), and particles about the density of water in a gas ($\epsilon=833$). In the case of gas bubbles, we do not account for the deformability of the bubbles or the deviation from Stokes drag due to a fluid disperse phase. Particle radius to gap widths ranged from $\phi=0.0002$ (the gap corresponds to 5000 particle diameters) to $\phi=0.02$ (the gap corresponds to 50 particle diameters). Assuming that the velocity difference between the particle and fluid is at least one order of magnitude smaller than the surface velocity of the inner cylinder (probably an overestimate), the particle Reynolds number is always less than 0.4 justifying the use of the Stokes drag in the formulation. Furthermore, a simple order of magnitude analysis of the ratio of the Bassett history force to the Stokes drag goes like ϕ, indicating that it is reasonable to neglect the particle history. Particle concentrations up to $A=0.05$ were considered, noting that our assumptions requiring a dilute concentration make our results most dependable at lower concentrations than this. Radius ratios from $\eta=0.45$ to $\eta=0.99$ were considered.

III. RESULTS AND DISCUSSION

The critical Taylor number for transition from stable cylindrical Couette flow to supercritical Taylor vortex flow for a suspension of neutrally buoyant particles is shown in Fig. 2 as a function of the particle concentration for radius ratios ranging from $\eta=0.45$ to $\eta=0.95$. As the particle concentration increases, the flow becomes less stable. For all conditions studied the critical Taylor number decreases by about

TABLE II. Critical wave numbers at different concentrations in the range $0 \leqslant A \leqslant 0.05$ for several radius ratios.

k_c (η=0.95)	k_c (η=0.85)	k_c (η=0.75)	k_c (η=0.65)	k_c (η=0.45)
3.127	3.130	3.135	3.143	3.172

7% as the particle concentration increases from zero to the maximum concentration. This result for spherical particles is different from theoretical predictions for rigid fibers.[30] In that case, the fibers stabilize the flow. The differing results could be a consequence of the different shape of the particles or the different analytical techniques (two-fluid model versus non-Newtonian rheological coefficients).

The critical wave number is not altered by the concentration of particles. Table II provides the wave number for neutrally buoyant particles for concentrations ranging from $A=0$ to $A=0.05$. This result is independent of density ratio and particle size ratio.

The effect of the particle density on the critical Taylor number is shown in Fig. 3 for three radius ratios. It is apparent that the more dense particles have a much greater effect on the stability of the flow than less dense particles. As the particle concentration increases from 0 to 5%, the decrease in the critical Taylor number is negligible for $\epsilon=0.001$, but as large as 35% for $\epsilon=10$. The destabilizing effect is even more striking for particles in a gas ($\epsilon=833$), where the critical Taylor number decreases to only a small fraction of its value as the particle concentration increases.

The greater effect of heavy particles on the stability may be attributed to their inertia, which results in an increased degree of coupling between the fluid and particle phases. This effect is most evident if considered in terms of the Stokes number, defined as

$$\mathrm{St}=\frac{\rho_p \phi^{*2} r_1 \Omega_1}{18 \mu d}.$$

The Stokes number represents the ratio of the viscous relaxation time for the particle ($\rho_p \phi^{*2}/18\mu$) to the time scale of the flow ($d/r_1\Omega_1$). It indicates the ability of the particles to respond to the motion of the carrier fluid.[40,51] For small values of the Stokes number, particles accurately follow the carrier fluid, whereas for large values the particles do not closely follow the fluid motion because of their inertia. The Stokes number for $\epsilon=833$ ranges from 10^{-2} to 10^{-1} depending on concentration and radius ratio, whereas for the lower density ratios, the Stokes number is one to six orders of magnitude less. Thus, for the smaller density ratios, the inertia of the particles is so small that the particles have little effect on the stability. For the largest density ratio, the particles interact more strongly with the flow and reduce the stability.

This naturally poses the possibility of accounting for the effect of the density ratio in the form of the critical Taylor number. The Taylor numbers in Figs. 2 and 3 are based on the fluid properties (density and viscosity). However, the presence of particles alters the effective density and viscosity of the suspension. This suggests the use of an effective Taylor number based on the bulk effective density and viscosity of the suspension. The effective density is readily calculated based on the particle concentration and the density ratio. The effective density can be as much as 42 times the fluid density for dense particles at the highest concentration considered. The effective viscosity is more difficult to specify. Several correlations, both theoretical and empirical, exist to calculate the effective viscosity of a suspension.[39] For simplicity, we use the Einstein formulation such that $\mu_{\mathrm{eff}}=\mu(1+2.5A)$. Thus, the effective viscosity can be as much as 12.5% greater than the fluid viscosity for the concentrations that we considered. Figure 4 indicates the dependence of the effective critical Taylor number, based on the effective bulk density and viscosity, on the concentration of particles for density ratios from $\epsilon=0.001$ to $\epsilon=833$ and the three radius ratios that were shown in Fig. 3. Using the effective critical Taylor number

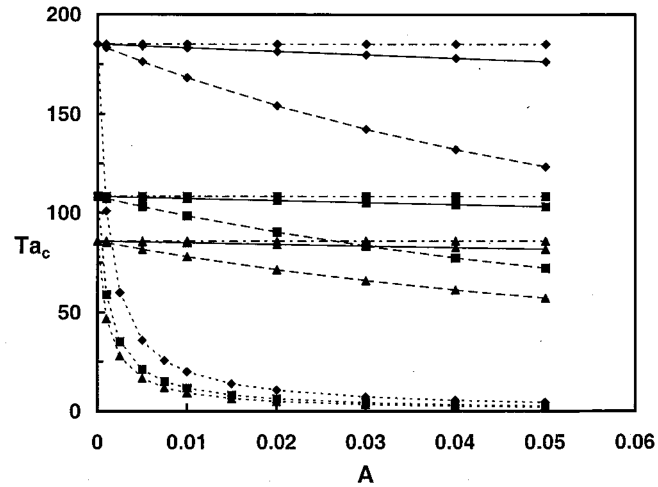

FIG. 3. The effect of density ratio ϵ on critical Taylor number for several radius ratios (— · —) $\epsilon=0.001$, (—) $\epsilon=1$, (– – –) $\epsilon=10$, (- - -) $\epsilon=833$; (▲) $\eta=0.75$, (■) $\eta=0.85$, (◆) $\eta=0.95$.

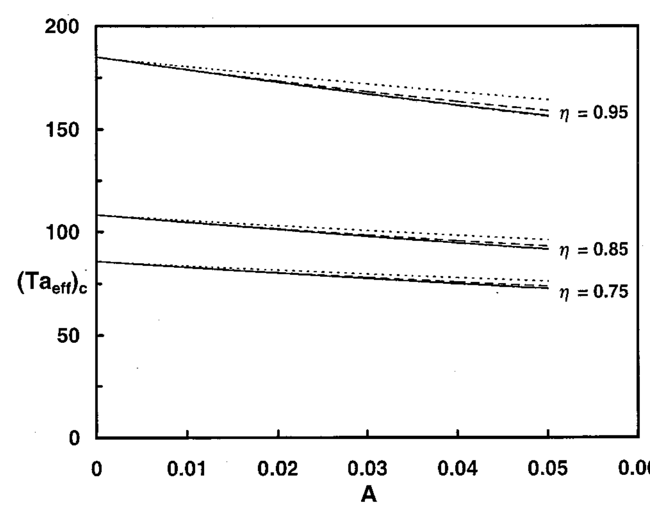

FIG. 4. The effect of particle concentration on the effective critical Taylor number. The effective Taylor number is based on the density and viscosity of the suspension (-·-) $\epsilon=0.001$ (nearly hidden by the solid line), (—) $\epsilon=1$, (–––) $\epsilon=10$, (---) $\epsilon=833$.

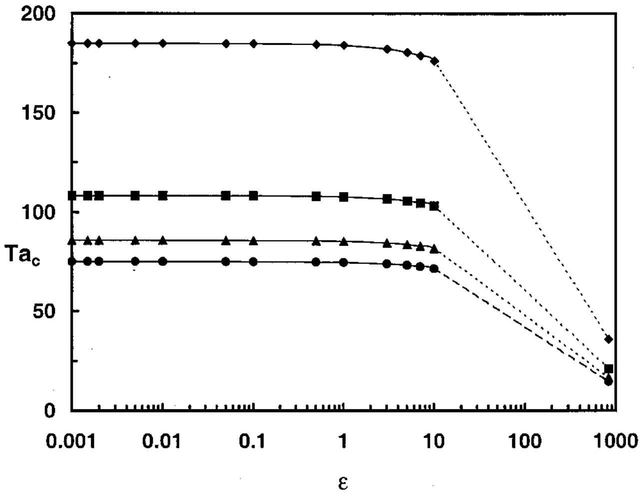

FIG. 5. Critical Taylor number as a function of density ratio for several radius ratios ($A=0.005$, $\phi=0.004$); (●) $\eta=0.65$, (▲) $\eta=0.75$, (■) $\eta=0.85$, (♦) $\eta=0.95$.

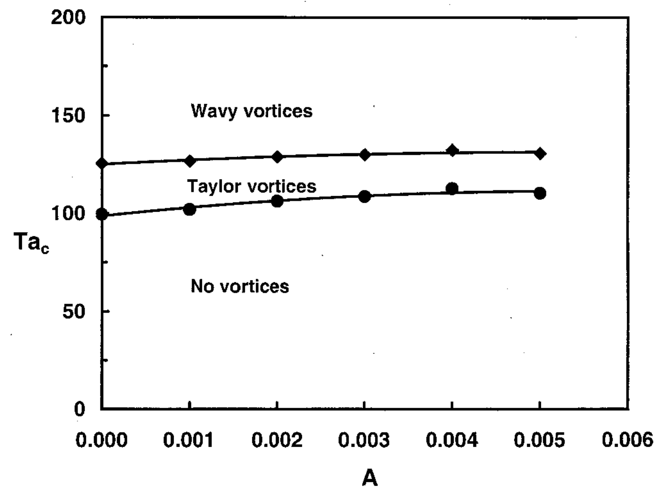

FIG. 6. Experimental results obtained using neutrally buoyant nylon particles ($\eta=0.824$, $\phi=0.0038$).

nearly collapses the data for this wide range of density ratios at all three radius ratios. Apparently, the effective suspension density, which plays a much greater role than the effective viscosity in the effective Taylor number, accounts for the degree to which particles follow the fluid flow and thereby affect the stability.

The effect of the density ratio ϵ on the critical Taylor number is shown in Fig. 5 for a single concentration of $A=0.005$ and several radius ratios. The density ratio has little effect on the critical Taylor number until it is quite large. (Values for $10<\epsilon<833$ were not calculated, since they do not represent physically realizable systems.)

Finally, we calculated the critical Taylor number for particle sizes of $0.0002\leqslant\phi\leqslant0.02$ over the range of concentrations and density ratios that were considered. The critical Taylor number and critical wave number were independent of ϕ.

IV. EXPERIMENTAL RESULTS FOR A NEUTRALLY BUOYANT SUSPENSION

We performed a limited number of experiments for suspensions of neutrally buoyant particles to determine how well the linear stability analysis captures the physics of the problem. The experiments were conducted using a standard Couette cell with a fixed outer cylinder, stepper motor driven inner cylinder, and fixed end caps such that $2r_1=4.97\pm0.013$ cm, $2r_2=6.03\pm0.013$ cm. The radius ratio was $\eta=0.824$ and the aspect ratio was $\Gamma=H/d=96$, where $H=50$ cm, is the height of the column. The concentration of the aqueous glycerol solution was matched to the approximate density of the nylon particles ($\rho\cong1.1$ g/cm^3). It was difficult to exactly match the density of all particles, due to variability in the particles. The 20 ± 5 μm particles (Goodfellow LS194265, Cambridge, UK) were used in volume concentrations of $0\leqslant A\leqslant0.005$. Surfactant in the form of detergent was added in very small amounts ($\cong$1.5 ml/1000 ml of suspension) to assure suspension of the particles. A small quantity ($A_{\text{flakes}}=0.000\,05$) of silicon dioxide coated mica reflective flakes (Flamenco Superpearl, Mearl Corp.) were added to the suspension to make the vortices visible. The concentration of the flakes was a factor of 20–100 times less than the nylon particle concentration. The temperature in the annulus was monitored during the experiments to permit temperature correction of the density and viscosity.

The Taylor number was increased from rest in a stepwise fashion using small increments ($\Delta\text{Ta}\approx1$ near the theoretical transition point). The system was allowed to equilibrate for at least 10 min after each change in Ta. Transition was said to occur at the minimum Taylor number where vortices were observed to fill the entire annulus. (Here we refer to the fluid Taylor number, not the effective Taylor number, though there is little difference between them for $\epsilon=1$.) Precursor vortices appeared first near the end caps and then in various parts of the annulus slightly below the critical Taylor number, consistent with previous results for simple fluids.[52] The Taylor number was increased until the vortices filled the annulus and then decreased until they were visible only in parts of the annulus. In this way, we could bracket the transition from stable to Taylor–Couette flow to be $98.6<\text{Ta}<100.3$ for $A=0$. The theoretical value is $\text{Ta}_c=100.73$ for the radius ratio of the setup.[50] Although the wavelength of the vortices was not measured precisely, it was clearly quite near the expected value for square vortical cells. When observing transition for nonzero particle concentrations, a similar method to bracket the transition was used to determine the critical Taylor number. The critical Taylor number for transition from Taylor vortex flow to wavy vortex flow was determined in a similar way. Transition to wavy vortex flow was said to occur when wavy vortices filled the entire annulus. For zero particle concentration the wavy transition could be bracketed as $1.24<\text{Ta}/\text{Ta}_c<1.25$. Previous experiments show significant variability in the transition depending on the aspect ratio and experimental conditions.[53] The range is 1.15 to 1.28 Ta_c for radius ratios near that in our experiments.

The effect of concentration on transition is shown in Fig.

6 for $A \leq 0.005$, concentrations that are much lower than the concentrations in previous figures. Clearly, the presence of neutrally buoyant particles stabilizes the flow for both the transition from stable flow to Taylor vortex flow and from Taylor vortex flow to wavy vortex flow. Obviously, the experimental results differ from the linear stability analysis. There may be a maximum in the data for $A = 0.004$ for both transitions with a slight downward trend for greater concentrations that might be consistent with the theoretical prediction. Unfortunately, the transition became more difficult to detect visually as the concentration increased, so that it was impossible to detect for $A > 0.005$. Thus, it is not clear if the maximum vaguely evident in Fig. 6 really occurs or is a result of the difficulty in identifying the transition to vortical flow at high particle concentrations. We further note that the experimental results displayed a consistent stabilizing trend with increasing concentration even for very low concentrations ($A = 0.001$).

We are confident that our experiments were repeatable and robust. While it was challenging to determine the exact Taylor number for transition by visualizing the flow, the stabilizing effect was quite clear. Our visual observation of the first transition coinciding with the predicted theoretical value for a fluid with no nylon particles gives us further confidence in our method. Furthermore, our visual observation of the transition to wavy vortices with no nylon particles is consistent with previous measurements. We note that it was quite difficult to match the fluid density to the particle density (a small fraction of the particles always sank while a similar small fraction floated). However, the bulk of the particles were neutrally buoyant, so we doubt that density differences affected the results.

There are some differences between the experiments and the stability analysis that could be speculated as reasons for the differing analytical and experimental results. (1) Although our experimental setup had a reasonably large aspect ratio, end effects, which are not included in the theory, could play a role. However, this seems unlikely given that end effects do not alter the critical Taylor number for particle-free flows except when the aspect ratio is quite small. (2) The model assumes monodisperse particles, whereas a reasonably narrow distribution of polydisperse particles were used in the experiments. However, the negligible dependence of the model results on particle size suggests that this is not a problem. (3) The model assumes spherical particles, whereas the experiments included flakes (in small concentration) for visualization and used particles that were not exactly spherical. Since similar flakes have been used by many researchers to visualize transition to vortical flow without adverse affects, we can only assume that the small concentration of flakes is inconsequential. (4) It is possible that the detergent added to aid in the dispersion of particles affected the stability of the flow. However, the amount of detergent was so small that the viscosity and density of the fluid were unaffected. Furthermore, the experiment at zero particle concentration using the water-glycerol-detergent solution matched the theoretical prediction quite well indicating no fluid non-Newtonian effects. The only possibility is that the detergent altered the interaction between phases so that the interfacial force term was altered from that used in Eq. (3). (5) The linear stability analysis necessarily neglects nonlinear terms. However, it seems unlikely that a subcritical instability related to these terms would occur altering the theoretical results. (6) The Bassett history force acting on the particles is assumed to be negligible based on an order of magnitude analysis. However, a recent study has suggested that the motion of a particle itself may be unstable when the Bassett history force is included.[54] The way in which this would impact the two-fluid model used here is unclear. (7) The linear stability analysis assumes that the stable concentration of particles is uniform [A in Eq. (5) is independent of r, z, and t]. Given the uniform shear in stable Couette flow, it seems unlikely that shear-induced diffusion would result in a concentration gradient, but clearly the wall-exclusion effect results in a nonuniform concentration profile near the walls of the annulus that was not included in the model. In addition, once vortices occur the concentration of particles is unlikely to be uniform. It is likely that one of the two latter points, the omission of history term or the assumption of a uniform concentration of particles in the theory, are the most likely causes of the theory not capturing the physics to properly match the experiments.

V. SUMMARY

The results of the theoretical analysis of the stability of a suspension in cylindrical Couette flow indicate that the flow is destabilized by the presence of a dispersed species. The degree of destabilization depends on the density ratio between the dispersed phase and the continuous phase. More dense particles result in more of a destabilizing effect. Most likely more dense particles (such as solid particles in a gas) are less likely to follow the fluid motion, based on the particle Stokes number. This results in a stronger interaction between the disperse and continuous phases through the Stokes drag term (since the velocity difference is greater). It is quite logical to argue that this disrupts the stability more easily than neutrally buoyant or very light particles. The effect of the density ratio can be readily taken into account, at least to a first approximation, by converting the calculated critical Taylor number, which is based on the fluid properties, to an effective Taylor number based on the bulk suspension density and viscosity. This permits the estimation of a critical Taylor number that is nearly independent of the density ratio. Nevertheless, our preliminary experiments with neutrally buoyant particles indicate a stabilizing effect of particles. This could be argued as a logical result given that the particles increase the effective viscosity slightly and thereby require a larger Taylor number based on fluid properties to have the effective Taylor number reach the critical value. However, this effect should be quite small for the experimental particle concentrations.

The original motivation for this work was the flow of suspensions in Taylor–Couette reactor cells or rotating filters. In these devices, the base flow is substantially more complex due to the necessary axial or radial flows to carry the process fluid into and out of the cell. The results presented here provide some insight with regard to these applications. In particular, our results suggest that an estimate of the conditions for the flow to become unstable may be based on the effective Taylor number. However, the differences between the experimental and theoretical results prevent any conclusions with regard to the stabilizing or destabilizing effect of particles in suspension on Taylor–Couette flow. Clearly, the effect of particles in suspension on the stability of Taylor–Couette flow remains an open question that has significance in several applications.

ACKNOWLEDGMENTS

Support by NASA and Northwestern University is gratefully acknowledged. M.E.A. acknowledges the research center of King Saud University for supporting this research. We thank Robert R. Smith for carrying out a simplified, preliminary derivation of the two-fluid stability problem.

[1] G. I. Taylor, ''Stability of a viscous liquid contained between two rotating cylinders,'' Philos. Trans. R. Soc. London, Ser. A **223**, 289 (1923).
[2] S. Chandrasekhar, *Hydrodynamic and Hydromagnetic Stability* (Oxford University Press, Oxford, 1961), pp. 272–342.
[3] R. C. DiPrima and H. L. Swinney, ''Instabilities and transition in flow between concentric rotating cylinders,'' in *Topics in Applied Physics, Hydrodynamic Instabilities and the Transition to Turbulence*, edited by H. L. Swinney and J. P. Gollub (Springer, Berlin, 1985), pp. 139–180.
[4] K. Kataoka, ''Taylor vortices and instabilities in circular Couette flows,'' in *Encyclopedia of Fluid Mechanics*, edited by N. P. Cheremisinoff (Gulf, Houston, 1986), Vol. 1, pp. 237–273.
[5] E. L. Koschmieder, *Benard Cells and Taylor Vortices* (Cambridge University Press, Cambridge, 1993).
[6] J. Kaye and E. C. Elgar, ''Modes of adiabatic and diabatic fluid flow in an annulus with an inner rotating cylinder,'' Trans. ASME **80**, 753 (1958).
[7] S. Chandrasekhar, ''The hydrodynamic stability of viscid flow between coaxial cylinders,'' Proc. Natl. Acad. Sci. U.S.A. **46**, 141 (1960).
[8] R. C. DiPrima, ''The stability of a viscous fluid between rotating cylinders with an axial flow,'' J. Fluid Mech. **9**, 621 (1960).
[9] S. K. Bahl, ''Stability of viscous flow between two concentric rotating porous cylinders,'' Def. Sci. J. **20**, 89 (1970).
[10] K. Bühler, ''Taylor vortex flow with superimposed radial mass flux,'' in *Ordered and Turbulent Patterns in Taylor–Couette Flow*, edited by E. D. Andereck and F. Hayot (Plenum, New York, 1992), pp. 197–203.
[11] K. Min and R. M. Lueptow, ''Hydrodynamic stability of viscous flow between rotating porous cylinders with radial flow,'' Phys. Fluids **6**, 144 (1994).
[12] R. D. Vigil, Q. Ouyang, and H. L. Swinney, ''Spatial variation of a short-lived intermediate chemical species in a Couette reactor,'' J. Chem. Phys. **96**, 6126 (1992).
[13] C. M. V. Moore and C. L. Cooney, ''Axial dispersion in Taylor–Couette flow,'' AIChE J. **41**, 723 (1995).
[14] R. J. Campero and R. D. Vigil, ''Spatio-temporal patterns in liquid–liquid Taylor–Couette–Poiseille flow,'' Phys. Rev. Lett. **79**, 3897 (1997).
[15] R. L. C. Giordano, R. C. Giordano, and C. L. Cooney, ''Performance of a continuous Taylor–Couette vortex flow enzymic reactor with suspended particles,'' Process Biochem. **35**, 1093 (2000).
[16] K. H. Kroner, V. Nissinen, and H. Ziegler, ''Improved dynamic filtration of microbial suspensions,'' Bio/Technology **5**, 921 (1987).
[17] K. H. Kroner and V. Nissinen, ''Dynamic filtration of microbial suspensions using an axially rotating filter,'' J. Membr. Sci. **36**, 85 (1988).
[18] G. Beaudoin and M. Y. Jaffrin, ''Plasma filtration in Couette flow membrane devices,'' Artif. Organs **13**, 43 (1989).
[19] S. Wronski, E. Molga, and L. Rudniak, ''Dynamic filtration in biotechnology,'' Bioprocess. Eng. **4**, 99 (1989).
[20] U. B. Holeschovsky and C. L. Cooney, ''Quantitative description of ultrafiltration in a rotating filtration device,'' AIChE J. **37**, 1219 (1991).
[21] G. Belfort, J. M. Pimbley, A. Greiner, and K. Y. Chung, ''Diagnosis of membrane fouling using a rotating annular filter. 1. Cell culture media,'' J. Membr. Sci. **77**, 1 (1993).
[22] G. Belfort, P. Mikulasek, J. M. Pimbley, and K. Y. Chung, ''Diagnosis of membrane fouling using a rotating annular filter. 2. Dilute particle suspensions of known particle size,'' J. Membr. Sci. **77**, 23 (1993).
[23] H. B. Winzeler and G. Belfort, ''Enhanced performance for pressure-driven membrane processes: The argument for fluid instabilities,'' J. Membr. Sci. **80**, 35 (1993).
[24] R. M. Lueptow and A. Hajiloo, ''Flow in a rotating membrane plasma separator,'' ASAIO J. **41**, 182 (1995).
[25] J. R. Hildebrandt and J. B. Saxton, ''The use of Taylor vortices in protein processing to enhance membrane filtration performance,'' in *Bioprocess Engineering Colloquium*, edited by R. C. Dean, Jr. and R. M. Nerem (American Society of Mechanical Engineers, New York, 1987), pp. 93–95.
[26] J. A. Schwille, D. Mitra, and R. M. Lueptow, ''Design parameters for rotating cylindrical filtration,'' J. Membr. Sci. (in press).
[27] R. G. Larson, ''Instabilities in viscoelastic flows,'' Rheol. Acta **31**, 213 (1992).
[28] R. E. Khayat, ''Onset of Taylor vortices and chaos in viscoelastic fluids,'' Phys. Fluids **7**, 2191 (1995).
[29] M.-K. Yi and C. Kim, ''Experimental studies on the Taylor instability of dilute polymer solutions,'' J. Non-Newtonian Fluid Mech. **72**, 113 (1997).
[30] B. Nsom, ''Transition from circular Couette flow to Taylor vortex flow in dilute and semiconcentrated suspensions of stiff fibers,'' J. Phys. II **4**, 9 (1994).
[31] J.-Y. Yuan and D. M. Ronis, ''Instability and pattern formation in colloidal-suspension Taylor–Couette flow,'' Phys. Rev. E **48**, 2880 (1993).
[32] D. S. Broomhead and S. C. Ryrie, ''Particle paths in wavy vortices,'' Nonlinearity **1**, 409 (1988).
[33] P. Ashwin and G. P. King, ''A study of particle paths in non-axisymmetric Taylor–Couette flows,'' J. Fluid Mech. **338**, 341 (1997).
[34] M. Rudman, ''Mixing and particle dispersion in the wavy vortex regime of Taylor–Couette flow,'' AIChE J. **44**, 1015 (1998).
[35] M. Rudolph, T. Shinbrot, and R. M. Lueptow, ''A model of mixing and transport in wavy Taylor–Couette flow,'' Physica D **121**, 163 (1998).
[36] S. T. Wereley and R. M. Lueptow, ''Inertial particle motion in a Taylor–Couette rotating filter,'' Phys. Fluids **11**, 325 (1999).
[37] K. Khellaf, G. Lauriat, and J. Legrand, ''Numerical tracking and circulation time distribution in an infinite Taylor system,'' Chem. Eng. Sci. **55**, 767 (2000).
[38] M. A. Dominguez-Lerma, G. Ahlers, and D. S. Cannell, ''Effects of 'Kalliroscope' flow visualization particles on rotating Couette–Taylor flow,'' Phys. Fluids **28**, 1204 (1985).
[39] M. Ungarish, *Hydrodynamics of Suspensions* (Springer, Berlin, 1993).
[40] A. A. Dimas and K. T. Kiger, ''Linear stability of a particle-laden mixing layer with a dynamic dispersed phase,'' Phys. Fluids **10**, 2539 (1998).
[41] M. R. Maxey and J. J. Riley, ''Equation of motion for a small rigid sphere in a nonuniform flow,'' Phys. Fluids **26**, 883 (1983).
[42] C. D. Andereck, S. S. Liu, and H. L. Swinney, ''Flow regimes in a circular Couette system with independently rotating cylinders,'' J. Fluid Mech. **164**, 155 (1986).
[43] M. R. Scott and H. A. Watts, ''Computational solution of linear two point boundary value problems via orthonormalization,'' SIAM (Soc. Ind. Appl. Math.) J. Numer. Anal. **14**, 40 (1977).
[44] K. L. Hiebert, SLATEC Common Math Library (National Energy Software Center, Argonne National Laboratory, Argonne, IL).
[45] M. J. D. Powell, *Numerical Methods for Nonlinear Algebraic Equations* (Gordon and Breach, New York, 1970).
[46] G. B. McFadden, S. R. Coriell, R. F. Boisvert, and M. E. Glicksman, ''Asymmetric instabilities in a buoyancy-driven flow in a tall vertical annulus,'' Phys. Fluids **27**, 1359 (1984).
[47] M. E. Ali, Doctoral thesis, University of Colorado-Boulder, 1988.
[48] M. E. Ali and P. D. Weidman, ''On the stability of circular Couette flow with radial heating,'' J. Fluid Mech. **220**, 53 (1990).
[49] M. E. Ali and P. D. Weidman, ''On the linear stability of cellular spiral Couette flow,'' Phys. Fluids A **5**, 1188 (1993).
[50] A. Recktenwald, M. Lücke, and H. W. Müller, ''Taylor vortex formation in axial through-flow: Linear and weakly nonlinear analysis,'' Phys. Rev. E **48**, 4444 (1993).
[51] R. P. Dring, ''Sizing criteria for laser anemometry particles,'' ASME J. Fluids Eng. **104**, 15 (1982).
[52] E. L. Koschmieder, *Benard Cells and Taylor Vortices* (Cambridge University Press, Cambridge, 1993).
[53] R. C. DiPrima, P. M. Eagles, and B. S. Ng, ''The effect of radius ratio on the stability of Couette flow and Taylor vortex flow,'' Phys. Fluids **27**, 2403 (1984).
[54] O. A. Druzhinin, ''On the stability of a stationary solution of the Tchen's equation,'' Phys. Fluids **12**, 1878 (2000).